DEVELOPMENTAL BIOLOGY **188,** 235–247 (1997)
ARTICLE NO. DB978664

# Haploinsufficient Phenotypes in *Bmp4* Heterozygous Null Mice and Modification by Mutations in *Gli3* and *Alx4*

**N. Ray Dunn,* Glenn E. Winnier,* Linda K. Hargett,† Jeffrey J. Schrick,‡ Agnes B. Fogo,§ and Brigid L. M. Hogan*,†,[1]**

**Department of Cell Biology, †Howard Hughes Medical Institute, and §Department of Pathology, Vanderbilt University Medical School, Nashville, Tennessee 37232-2175; and ‡Children's Hospital Research Foundation, Division of Developmental Biology, Cincinnati, Ohio 45229*

***Bone morphogenetic protein 4* (*Bmp4*), a vertebrate homolog of *Drosophila decapentaplegic* (*dpp*), encodes a signaling protein with multiple functions during embryogenesis. Most mouse embryos homozygous for the $Bmp4^{tm1blh}$ null allele die around the time of gastrulation, with little or no mesoderm. Two independently derived $Bmp4^{tm1}$ mutations were backcrossed onto the C57BL/6 genetic background. Several independently expressed, incompletely penetrant abnormalities were observed in heterozygotes, including cystic kidney, craniofacial malformations, microphthalmia, and preaxial polydactyly of the right hindlimb. In addition, heterozygotes were consistently underrepresented at weaning. These results indicate that *Bmp4* gene dosage is essential for the normal development of a variety of organs and for neonatal viability. Two mutations that enhance the penetrance and expressivity of the polydactylous phenotype were identified: $Gli3^{XtJ}$, a deletion mutation involving a gene encoding a zinc-finger protein related to *Drosophila* cubitus interruptus, and $Alx4^{tm1rwm}$, a targeted null mutation in a gene encoding a paired class homeoprotein related to *Drosophila* aristaless. All double $Bmp4^{tm1}$; $Gli3^{XtJ}$ heterozygotes have extensive anterior digit abnormalities of both fore- and hindlimbs, while all double $Bmp4^{tm1}$; $Alx4^{tm1}$ heterozygotes display ectopic anterior digits only on the hindlimbs. These genetic interactions suggest a model for the multigenic control of anterior digit patterning during vertebrate limb development.** 

## INTRODUCTION

The establishment of a three-dimensional pattern within embryonic tissues is regulated by secreted signaling proteins belonging to a number of evolutionarily conserved families, including the Wnts, Hedgehogs (Hhs), fibroblast growth factors (FGFs), and transforming growth factors (TGF$\beta$s). In the case of the TGF$\beta$/bone morphogenetic protein (BMP) superfamily, there is contrasting evidence that the proteins either act locally within a few cell diameters of the ligand source (Jones *et al.*, 1996; Reilly and Melton, 1996) or establish gradients of activity, and thereby function as true morphogens (Wharton *et al.*, 1993; Gurdon *et al.*, 1994; Lecuit *et al.*, 1996; Nellen *et al.*, 1996). Whatever the precise mechanism, the amount of BMP secreted by a signaling source appears to be important for achieving the appropriate response in a target tissue. This conclusion is based in part on the finding that some heterozygous null mutants, which presumably produce half the amount of active BMP protein as wild type, show significant patterning defects.

The best evidence of a BMP-related haploinsufficient phenotype comes from studies of dorsal–ventral (D-V) patterning in *Drosophila*. In the blastoderm embryo, *decapentaplegic* (*dpp*) is transcribed uniformly over the dorsal half of the embryo (St. Johnston and Gelbart, 1987). Embryos homozygous for null *dpp* mutations are completely ventralized and 100% die. Heterozygous null mutants exhibit a high percentage of dominant lethality, showing that the remaining wild-type allele does not produce enough active Dpp to meet the early D-V requirement (Irish and Gelbart, 1987). Other partial loss-of-function *dpp* alleles display

[1] To whom correspondence should be addressed at Howard Hughes Medical Institute, Vanderbilt University School of Medicine, C-2310 Medical Center North, Nashville, TN 37232-2175. Fax: 615.343.2033. E-mail: brigid.hogan@mcmail.vanderbilt.edu.

0012-1606/97 $25.00

lower incidences of dominant lethality and result in slight deletions of dorsally derived structures (Irish and Gelbart, 1987; Wharton *et al.*, 1993). These observations are consistent with a model in which cell fate is specified along the D-V axis according to a graded distribution of Dpp activity (Ferguson and Anderson, 1992a; Wharton *et al.*, 1993). Of relevance to the findings in this paper, similar models for a Dpp activity gradient have been proposed for the *Drosophila* wing and leg imaginal discs (Lecuit *et al.*, 1996; Nellen *et al.*, 1996; Singer *et al.*, 1997; Goto and Hayashi, 1997).

Several mutations have been identified that modify the phenotype of weak *dpp* alleles; these include mutations in the genes *Mothers against decapentaplegic* (*mad*), *medea*, and *tolloid* (*tld*) (Ferguson and Anderson, 1992a,b; Raftery *et al.*, 1995). Characterization of these genes and their products has lead to new information about the downstream signaling pathways activated by Dpp and about the extracellular proteins that modify Dpp activity. Thus, the identification of genetic modifiers provides an important inroad to the understanding of the cellular and genetic interactions underlying embryonic development (Erickson, 1996; Winter, 1996).

There is good evidence that BMP5 functions in a dose-dependent manner during embryonic development. Mice homozygous for the classical *short ear* ($Bmp5^{se}$) mutation show a broad range of skeletal malformations, including the loss of serveral small bones, lung cysts, hydroureter and hydronephrosis, and a characteristic reduction in external ear size (Green, 1968; Kingsley *et al.*, 1992). $Bmp5^{se}$ heterozygotes display less severe soft tissue defects and only a slight reduction in overall skeletal size (Green, 1968). Although the etiology of the abnormalities in $Bmp5^{se}/Bmp5^{se}$ and $Bmp5^{se}/+$ mutant mice is still unknown, *Bmp5* is expressed in all the affected organs during embryogenesis and in regions of condensing prechondrogenic cells early in the process of endochondral bone formation (King *et al.*, 1994). Furthermore, the phenotypes of $Bmp5^{se}$ mutant mice are dependent upon as yet unidentified strain-specific genetic modifiers (Green, 1957). Taken together, these observations suggest that the amount of active BMP5 is critical for the normal development of a wide range of organ systems.

*Bmp4* is also expressed in many tissues during mouse development (Jones *et al.*, 1991; Winnier *et al.*, 1995; Bitgood and McMahon, 1995; for review Hogan, 1996). For example, at the 8 somite stage (8.5 days postcoitum (p.c.)), *Bmp4* transcripts are localized in the lateral mesoderm around the fore- and hindgut and the posterior primitive streak mesoderm, as well as in the allantois, amnion, and early heart. During later development, *Bmp4* is expressed in a dynamic pattern in both the mesenchyme and apical ectodermal ridge (AER) of the limb bud and many other sites, including the facial processes, the lung, the kidney, the fore- and hindbrain, and localized regions of the optic cup and retinal epithelium of the developing eye (Jones *et al.*, 1991; Francis *et al.*, 1994; Bellusci *et al.*, 1996; Hogan, 1996; Dudley and Robertson, 1997; Barlow and Francis-West, 1997; Furuta *et al.*, 1997; N.R.D. and B.L.M.H., unpublished observations). We have previously reported the early embryonic lethality of mouse embryos homozygous for a targeted null mutation in *Bmp4* (Winnier *et al.*, 1995). Although some survive to the early forelimb bud stage, most homozygous mutant embryos die at gastrulation (~6.5 days p.c.), with little or no mesoderm formation. In order to study the effect of genetic background on this variable mutant phenotype, we backcrossed the mutation onto C57BL/6. From the third backcross generation, consistent defects in several organ systems were observed at low penetrance in heterozygotes, including preaxial hindlimb polydactyly. In addition, compared to their wild-type littermates, $Bmp4^{tm1}/+$ pups were underrepresented at weaning, suggesting a requirement for diploid gene dosage for neonatal viability. Finally, two genetic modifiers (enhancers) of the $Bmp4^{tm1}/+$ polydactylous limb phenotype, $extra\text{-}toes^{J}$ ($Gli3^{Xtj}$) and $Alx4^{tm1}$, have been identified, and models for how these interactions occur are proposed.

## MATERIALS AND METHODS

### Mice

Production of the null $Bmp4^{tm1blh}$ mutation in D3 embryonic stem (ES) cells (derived from 129/Sv embryos in 1985) and its backcross onto C57BL/6NHsd (Harlan Sprague–Dawley, Indianapolis, IN) have been previously reported (Winnier *et al.*, 1995). This line is called B286. To generate a second line of $Bmp4^{tm1}$ mice, TL1 ES cells (recently derived from 129/SvEvTacfBR embryos; Taconic, Germantown, NY) at passage 11 were electroporated as described, and drug-resistant clones were screened with 5′ external and internal and 3′ external probes (Winnier *et al.*, 1995). A correctly targeted clone, 1A10H, was injected into C57BL/6 blastocysts. Germline chimeras were bred to C57BL/6NHsd females, and the backcross was carried out as above.

Heterozygous $Gli3^{Xtj}$ males (C57BL/6J-$Gli3^{Xtj}$) from The Jackson Laboratory (Bar Harbor, ME) were mated to C57BL/6NHsd females. Heterozygous offspring were identified at weaning by preaxial digit abnormalities. Homozygous embryos were easily identified by their forebrain abnormalities, reduced eye size, and paddle-shaped limb buds from 10.5 days p.c.

Mice heterozygous for a targeted null mutation in the *Aristaless-like homeobox 4* (*Alx4*) gene on a 129/J genetic background were kindly provided by Drs. Shimian Qu and Ronald Wisdom, Vanderbilt University Medical School (Qu *et al.*, submitted for publication). For convenience, the targeted *Alx4* allele is unofficially designated $Alx4^{tm1}$ throughout this paper.

### DNA Extraction and Genotyping

The $Bmp4^{tm1}$ allele was identified by Southern blot analysis as described (Winnier *et al.*, 1995) with modifications (Laird *et al.*, 1991). In addition, genotypes were determined by PCR amplification of a 500-bp region within the MC1neopA cassette (Soriano *et al.*, 1991). Primers were 5′-GGA CTG GCT GCT ATT GGG CGA AGT G-3′ and 5′-GAA GAA CTC GTC AAG AAG GCG ATA GAA GG-3′ (25 cycles with an annealing temperature of 61°C). Wild-type and $Alx4^{tm1}$ alleles were distinguished by PCR analysis of genomic DNA as described (Qu *et al.*, submitted for publication).

**TABLE 1**

Genotypes of Offspring from the *Bmp4$^{tm1}$* Backcross onto C57BL/6

| *Bmp4$^{tm1}$* × C57BL/6 | | | |
|---|---|---|---|
| | | Genotype[a] | |
| Line | Sex | +/+ | *Bmp4$^{tm1}$*/+ |
| B286[b] | Male | 224 | 151 |
| | Female | 197 | 70 |
| | Total (%) | 421 (66%) | 221 (34%) |

[a] Genotypes were determined at weaning (approximately 3 weeks) for pups born between the N6 and N13 backcross generations.

[b] This is the name given to the *Bmp4$^{tm1}$* line derived from D3 ES cells.

**TABLE 2**

Phenotypes Observed in *Bmp4$^{tm1}$* Heterozygotes during the Backcross onto C57BL/6

| Abnormality[a] | +/+ with defect[b] (total) | +/− with defect[b] (total) |
|---|---|---|
| Cystic kidney | 2/190 (1%) | 13/113 (12%) |
| Hind limb polydactyly | 0/358 (0%) | 26/209 (12%) |
| Eye defects | 37/346 (11%) | 66/186 (35%) |
| Craniofacial defects | 16/342 (5%) | 22/188 (12%) |
| Male accessory glands | 0/217 (0%) | 8/118 (7%) |
| Circling | 4/358 (1%) | 14/209 (7%) |

[a] The phenotypes listed here were independently variably penetrant, i.e., not all animals had multiple defects.

[b] The data shown here represent the observations made between the N6 and N13 backcross generations, for which the most detailed records are available. Data on the frequency of eye defects in wild-type mice were also obtained from Harlan Sprague–Dawley.

### *Skeletal Preparations and Kidney Histology*

Cartilage and bone were stained, respectively, with Alcian blue 8 GX (Sigma) and alizarin red S (Sigma) (Selby, 1987; McLeod, 1980). Kidneys were fixed in 4% paraformaldehyde and PBS, dehydrated, and embedded in wax. Sections (7 $\mu$m) were stained with Masson stain.

### *Whole-mount in Situ Hybridization*

*In situ* hybridization was as described (Winnier *et al.*, 1995). Digoxigenin-labeled riboprobes for *Bmp4* were transcribed by T7 polymerase from the 1.5-kb full-length mouse cDNA. *Msx1* and *Msx2* riboprobes were transcribed by T7 polymerase from ~1-kb cDNA fragments and for *Sonic hedgehog* (*Shh*) by T3 polymerase from a 642-bp cDNA fragment.

### *Cell Death*

Dissected embryos were stained in a solution of 0.005% Nile blue sulfate (Sigma) in PBS or Tyrode's solution for 30 min at 37°C and then washed in prewarmed PBS and stored in 4% paraformaldehyde at 4°C until photography.

## RESULTS

### *Incompletely Penetrant, Postnatal Lethality of Heterozygous Bmp4$^{tm1}$ Mice*

Male germ-line chimeras from the B286-targeted ES cell line were mated to C57BL/6NHsd females, and heterozygous males serially backcrossed to C57BL/6 females (Winnier *et al.*, 1995). Of the 642 mice genotyped at weaning between the N6 and N13 backcross generations, only 34% were *Bmp4$^{tm1}$*/+, and, among these, females were significantly underrepresented (Table 1). Comparison of litter size at birth and weaning showed that 25% of the pups were lost postnatally. The reduced viability of *Bmp4$^{tm1}$* heterozygotes was confirmed by genotyping neonates, which showed approximately equal numbers of heterozygous and wild-type pups at birth (data not shown and Table 3).

### *Defects in Kidney, Male Accessory Glands, and Eye in Bmp4$^{tm1}$/+ Animals*

As the backcross progressed, several defects were observed in both male and female heterozygotes (Table 2). Those described here are for the B286 line, but have been subsequently confirmed with a second line, as described

**TABLE 3**

Genotypes of Offspring from the *Bmp4$^{tm1}$* × *Gli3$^{XtJ}$* Cross

| *Bmp4$^{tm1}$*/+ × *Gli3$^{XtJ}$*/+ | | |
|---|---|---|
| | Line | |
| | B286[a] | 1A10H[b] |
| Genotype | Number (% total) | Number (% total) |
| +/+; +/+ | 38 (36%) | 28 (28%) |
| +/+; *Gli3$^{XtJ}$*/+[c] | 32 (30%) | 24 (24%) |
| *Bmp4$^{tm1}$*/+; +/+ | 16 (15%) | 26 (26%) |
| *Bmp4$^{tm1}$*/+; *Gli3$^{XtJ}$*/+ | 20 (19%) | 21 (21%) |
| Total | 106 | 99 |

[a] Male B6.129-*Bmp4$^{tm1}$* (N8) heterozygotes were mated to female *Gli3$^{XtJ}$*/+. Tail biopsies were collected at weaning for *Bmp4* genotyping.

[b] Male B6.129-*Bmp4$^{tm1}$* (N2) heterozygotes were mated to female *Gli3$^{XtJ}$*/+. Tail biopsies were collected at birth (Postnatal Day 0 (P0)) or P1 for *Bmp4* genotyping.

[c] *Gli3$^{XtJ}$*/+ heterozygotes were identified by the presence of preaxial digit abnormalities on the fore- and/or hindlimb.

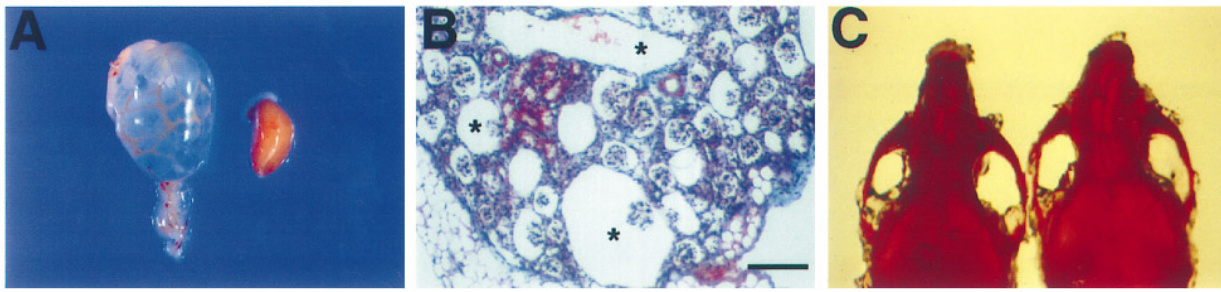


**FIG. 1.** Kidney and craniofacial defects in heterozygotes. (A) Cystic and normal contralateral kidney from an adult *Bmp4*$^{tm1}$/+ mouse. (B) Section through residual tissue of a similar hydronephrotic kidney, showing glomerulocystic abnormalities. Asterisks indicate dilated Bowman's space surrounding glomeruli. Scale bar, 50 $\mu$m. (C) Skulls of wild-type (left) and *Bmp4*$^{tm1}$/+ (right) adult mice stained with alizarin red, showing asymmetric shortening of the nasal bones in the heterozygote.

later. Of the *Bmp4*$^{tm1}$/+ adults examined, 12% displayed a single cystic kidney, with no left–right preference (Table 2; Fig. 1A). In most of the affected animals, there was marked hydronephrosis without dilation of the ureter. The remaining kidney cortex was atrophic with multiple, predominantly cortical, cysts, involving both tubules and glomeruli (Fig. 1B). In kidneys with less severe hydronephrosis, these cystic changes predominated, with dilation of Bowman's space surrounding the glomeruli (asterisks in Fig. 1B). Glomerular development appeared normal. Tubules showed occasional cystic changes as well, with interspersed intact tubules and mild interstitial fibrosis (Fig. 1B).

Abnormalities were also observed in male accessory glands (Table 2). These included cystic coagulating glands and seminiferous tubules, occasionally with abnormal lobulation. *Bmp4*$^{tm1}$/+ mice also exhibited a threefold greater frequency of microphthalmia and anophthalmia compared to the normal frequency of congenital eye abnormalities in wild-type C57BL/6 mice (Table 2). Some *Bmp4*$^{tm1}$ heterozygotes (7%) circled continuously in their cages, possibly as a result of inner ear or neurological defects (not analyzed further).

## *Defects in Skeletal Development*

In 12% of heterozygous males and females, the frontal and nasal bones were shorter, often curving unilaterally to give the appearance of a ''boxer's nose'' (Table 2; Fig. 1C). This craniofacial malformation was often associated with slight malocclusion. Malocclusion was observed in only 5% of wild-type C57BL/6 mice (Table 2), but was not associated with obvious skull abnormalities. In addition, 12% of *Bmp4*$^{tm1}$ heterozygotes exhibited unilateral anterior (preaxial) polydactyly, restricted to the right hindlimb. In approximately 70% of the affected specimens, two digits extended from metatarsal I (Fig. 2B). The most anterior digit resembled digit II, as determined by the presence of three phalanges (Fig. 2B). The remaining 30% showed either a biphalangeal ectopic digit (Fig. 4B) or an amorphous preaxial ossified nubbin (Fig. 2C). This partially penetrant, variably expressive polydactyly occurred in each backcross generation from N3 and at a constant frequency between generations N6 to N13, for which the most detailed breeding records are available. Neither fore- nor hindlimb polydactyly was seen in parental C57BL/6NHsd mice or in wild-type littermates.

## *Genetic Interaction between Bmp4*$^{tm1}$ *and Gli3*$^{XtJ}$

To search for mutations that modify this heterozygous polydactylous phenotype, we crossed *Bmp4*$^{tm1}$ heterozygotes with mice heterozygous for a null mutation in *Gli3*, a member of a family of mammalian genes—*Gli*, *Gli2*, and *Gli3*—that encodes a zinc-finger DNA-binding protein homologous to *Drosophila* cubitus interruptus (Ci) (Kinzler *et al.*, 1988; Ruppert *et al.*, 1988; Orenic *et al.*, 1990; Hui *et al.*, 1994). This choice was prompted by studies in *Drosophila* showing that Ci regulates the expression of *dpp*, the fly homolog of *Bmp4* (Alexandre *et al.*, 1996; Domínguez *et al.*, 1996; Hepker *et al.*, 1997). *Gli3* is expressed in multiple regions of the developing mouse embryo, including the limb bud mesenchyme (Schimmang *et al.*, 1992; Hui and Joyner, 1993; Hui *et al.*, 1994; Büscher *et al.*, 1997; Masuya *et al.*, 1997; Mo *et al.*, 1997). Several semidominant mutations of *Gli3* have been characterized: *Gli3*$^{Xt}$, *Gli3*$^{XtJ}$, *Gli3*$^{bph}$, and *Gli3*$^{Pdn}$ (Johnson, 1967, 1969; Hui and Joyner, 1993; Schimmang *et al.*, 1994). Homozygous *Gli3* mutants typically die before birth, with extreme hyperphalangy, a high incidence of midbrain exencephaly, misplaced ears, and poorly developed eyes. Heterozygous *Gli3* mutants show forefoot abnormalities and preaxial polydactyly of the hindfeet, with almost complete penetrance and variable expressivity. Both the homozygous and heterozygous *Gli3* mutant phenotypes vary with genetic background. For our experiments, we used the *Gli3*$^{XtJ}$ allele, a spontaneous mutation involving an intragenic deletion of at least 30 kb in the *Gli3* gene. This mutation was maintained on the


**FIG. 2.** Hindlimb defects in *Bmp4*$^{tm1}$/+, *Gli3*$^{XtJ}$/+, and *Bmp4*$^{tm1}$/+; *Gli3*$^{XtJ}$/+ adult mice on the C57BL/6 background. All panels show dorsal views of right hindlimbs stained with alizarin red. (A) Wild type; digit I is anterior and V posterior. (B and C) *Bmp4*$^{tm1}$/+ limbs display a range of incompletely penetrant digit abnormalities. The predominant phenotype is an additional triphalangeal digit (II* in B); an ectopic amorphous nubbin (arrowhead in C) is rarely observed. (D–F) *Gli3*$^{XtJ}$ heterozygotes show similar digit defects, including digit I duplications (I* in D and E) and ectopic ossified nubbins (arrowhead in F). (G–L) Double heterozygotes exhibit a more severe hindlimb polydactyly. The region anterior to digit III is grossly disorganized, with as many as three extra digits, connected by soft tissue syndactyly (arrowheads in G, J). Digit II is typically shifted laterally or ventrolaterally. The proximal phalange of digit II (P3 in L) and, in some specimens, the proximal phalange of a supernumerary digit (P3* in J) are irregularly shaped and project two closely apposed digits. In 100% of the *Bmp4*$^{tm1}$/+; *Gli3*$^{XtJ}$/+ hindlimbs, ectopic (M* in G, H, J, K) or malformed (M* in I, L) metatarsals are observed. In some cases, these extend two digital extremities (H, I, K, L).

C57BL/6 inbred background, i.e., the same background as the *Bmp4*$^{tm1}$ mutation.

The hindlimbs of C57BL/6-*Gli3*$^{XtJ}$/+ mice showed the following defects in order of frequency (488 limbs examined): preaxial amorphous ossified nubbins along the axis or at the base of digit I (58%, Fig. 2F); partial to complete duplications of digit I, as determined by the number of phalanges (8%, Figs. 2D and 2E); and polysyndactyly of digit I (2%, data not shown). The most common forelimb heterozygous phenotype (54%) was the circular flexure of digit II either toward the ventral footpad or toward the rudimentary thumb (digit I) (Fig. 3F). Less frequently (20%), the thumb appeared thickened and was connected to the curved digit II by soft tissue syndactyly with no bone fusion (Fig. 3F). Rarely (2%), the most distal phalange of digit II was duplicated (Fig. 3F). Multiple limbs could be affected in an individual, with no left or right, fore- or hindlimb prevalence. Furthermore, the phenotypes were seen equally in both males and females.

Since *Gli3*$^{XtJ}$/+ and *Bmp4*$^{tm1}$/+ both display preaxial polydactylous phenotypes, *Bmp4* and *Gli3* may participate in common or parallel genetic pathways that regulate anterior digit patterning in the early limb bud. To address these possibilities, B6.129-*Bmp4*$^{tm1}$ males (N8; 99.2% homozygosity of the C57BL/6 genome) from the B286 line were mated to female C57BL/6-*Gli3*$^{XtJ}$/+ mice (Table 3). Consistent with our previous findings, *Bmp4*$^{tm1}$ heterozygotes were again underrepresented in the F1 generation. Among the 35 *Bmp4*$^{tm1}$/+; +/+ animals obtained, no preaxial polydactyly was observed, which was consistent with the low penetrance of the heterozygous phenotype. However, 100% of the 20 double *Bmp4*$^{tm1}$; *Gli3*$^{XtJ}$ heterozygotes showed exacerbated preaxial digit defects on both of the fore- and hindfeet. Although the double heterozygous phenotypes were variably expressive, several consistent defects were seen. First, the digit abnormalities were restricted to the preaxial side of the hindfeet and involved only digits I and II; digits III–V were never affected (Figs. 2G–2L). Second, in contrast to both single heterozygotes, defects were seen in the metatarsals of double heterozygotes. Metatarsal I was often misplaced ventrally (Figs. 2G, 2H, 2J, and 2K) and, in more severe cases, had an irregular jagged shape (Fig. 2I and

out of view in 2L). In most $Bmp4^{tm1}/+$; $Gli3^{XtJ}/+$ hindfeet, ectopic club-shaped metatarsals were found either anterior to metatarsal I or between metatarsals I and II (Figs. 2G, 2H, 2J, and 2K). In a few affected individuals, the distal end of metatarsal I or II was trapezoidal and extended two, rather than one, terminal phalange (Figs. 2I and 2L). Third, digits I and II often showed irregular growth, with intervening extra digits. The ectopic digits contained varying numbers of phalanges of abnormal length and size, occurred with corresponding ventral sesamoid bones, and appeared as digit I or II duplications (data not shown and Figs. 2G–2L). In addition, the native and ectopic digits were often closely apposed and, in most instances, were connected by soft tissue syndactyly (Fig. 2G). Finally, no consistent mirror image symmetry of digit identity was observed.

### *Heterozygous Mutant Phenotype and Genetic Interaction with $Gli3^{Xtj}$ Are Seen with Two Independent $Bmp4^{tm1}$ Mutant Lines*

The initial $Bmp4^{tm1}/+ \times Gli3^{Xtj}/+$ cross was carried out with B6.129-$Bmp4^{tm1}$ (N8) mice of the B286 line. At the eighth backcross generation, theoretically 25 c*M* 129/Sv DNA still surrounds the *Bmp4* locus (Silver, 1995). It is therefore possible that the polydactyly seen in heterozygotes from the B286 line is due to a spontaneous semidominant mutation in a locus tightly linked to *Bmp4*. Therefore, a second line of $Bmp4^{tm1}$ mice (1A10H) was generated in different ES cells. In this new line, two heterozygous mice exhibited unilateral right hindlimb polydactyly at the third backcross generation (N3) to C57BL/6 (data not shown). We conclude that the $Bmp4^{tm1}$ mutation is solely responsible for the heterozygous phenotype.

To generate double heterozygotes from the 1A10H line, B6.129-$Bmp4^{tm1}$ (N2) (50% homozygosity of the C57BL/6 genome) males were mated to female $Gli3^{Xtj}/+$ (Table 3). Double heterozygous neonates displayed variably exacerbated fore- and hindlimb polydactyly identical to the polydactyly described for adults of the B286 line (above and Fig. 3). In order to examine this polydactyly in more detail, skeletons from neonates were examined after staining for cartilage and bone. In 1A10H $Bmp4^{tm1}/+$; $Gli3^{Xtj}/+$ hindlimbs, ectopic metatarsals were seen between metatarsals I and II and projected articulated extra digits resembling digit I (Figs. 3C and 3D). In Fig. 3C, digit I is bifurcated with fusion between adjacent phalanges. In contrast, the specimen in Fig. 3D showed a digit I duplication, but the distal phalanges were not fused. The forelimbs of a typical 1A10H $Bmp4^{tm1}$; $Gli3^{Xtj}$ double heterozygote are shown in Figs. 3G and 3H. The cartilaginous precursors of the rudimentary thumb were lengthened and bifurcated, with syndactyly of the distal phalange. Both forelimbs displayed the characteristic digit II $Gli3^{Xtj}/+$ flexure (Fig. 3F), with the addition of an ectopic digit between the thumb and digit II (Figs. 3G and 3H). Although duplications of the distal phalange of digit II were seen among more severely affected $Gli3^{Xtj}/+$ forelimbs (Fig. 3F), duplications of the digit axis as well as postaxial nubbins were not observed (data not shown and Fig. 3H). Last, the forelimb abnormalities of both 1A10H and B286 $Bmp4^{tm1}$; $Gli3^{Xtj}$ double heterozygotes were very similar (data not shown).

### *Genetic Interactions between $Bmp4^{tm1}$ and $Alx4^{tm1}$*

The *Alx4* gene, which encodes a paired class homeoprotein similar to *Drosophila aristaless*, is expressed in the anterior mesenchyme of the limb bud, as well as in other mesodermal tissues of the mouse embryo (Qu *et al.*, submitted for publication). Nearly all homozygous null $Alx4^{tm1}$ embryos die soon after birth, with a herniated gut and striking preaxial polydactyly of all four limbs. No heterozygous defects are observed. The extra digits are triphalangeal, suggesting a more posterior character, for example digits II or III (Fig. 4C). This polydactyly is reminiscent of the $Bmp4^{tm1}$ heterozygous phenotype described above, suggesting that *Alx4* interacts directly or indirectly with *Bmp4* to pattern the anterior of the limb bud. To test this hypothesis, B6.129-$Bmp4^{tm1}$ (N2) males were mated to coisogenic 129/J-$Alx4^{tm1}/+$ females, and 129/J-$Alx4^{tm1}/+$ males were mated to 129/Sv-$Bmp4^{tm1}$ females (Table 4). Three $Bmp4^{tm1}$ newborn heterozygotes from this cross exhibited unilateral right hindlimb polydactyly, consistent with the low penetrance of this phenotype (Fig. 4B). However, all 12 double $Bmp4^{tm1}$; $Alx4^{tm1}$ heterozygotes showed bilateral preaxial hindlimb polydactyly (Figs. 4C and 4D). In contrast to the $Bmp4^{tm1}/+$ polydactyly, the extra digit in $Bmp4^{tm1}$; $Alx4^{tm1}$ mutants extended from a duplicated metatarsal (Figs. 4B–4D). Furthermore, the extra digit was triphalangeal and longer than digit I. Although the anterior duplicated digit resembled digits II and III (Figs. 4C and 4D), we cannot conclude that it actually represents a mirror-symmetric duplication. In addition to the hindlimb defects, postaxial nubbins were observed on the forelimbs in 80% of the double $Bmp4^{tm1}$; $Alx4^{tm1}$ heterozygous mutants (data not shown).

### *Bmp4 and Msx1/2 Gene Expression in $Gli3^{Xtj}/Gli3^{Xtj}$ and $Alx4^{tm1}/Alx4^{tm1}$ Embryonic Limbs*

One explanation for the enhanced limb polydactyly of $Bmp4^{tm1}$; $Gli3^{Xtj}$ and $Bmp4^{tm1}$; $Alx4^{tm1}$ double heterozygotes is that Gli3 and Alx4 positively regulate *Bmp4* RNA levels. This hypothesis is supported by the overlapping expression patterns of *Bmp4*, *Gli3*, and *Alx4* in the anterior region of the developing limb bud beginning at 10.5–11.0 days p.c. We therefore examined the expression of *Bmp4* in $Gli3^{Xtj}/Gli3^{Xtj}$ and $Alx4^{tm1}/Alx4^{tm1}$ homozygous embryos. At 12.0–12.5 days p.c (Figs. 5A–5C), no obvious change in the level or distribution of *Bmp4* RNA was observed in either $Gli3^{Xtj}$ or $Alx4^{tm1}$ homozygous limbs, as judged by whole-mount *in situ* hybridization. Similar results were seen from 10.5 to 13.5 days p.c (data not shown).

Alternatively, it is possible that Gli3 and Alx4 are components of the BMP4 downstream signaling pathway, positively regulating such genes as *Msx1* and *Msx2* (Vainio *et*

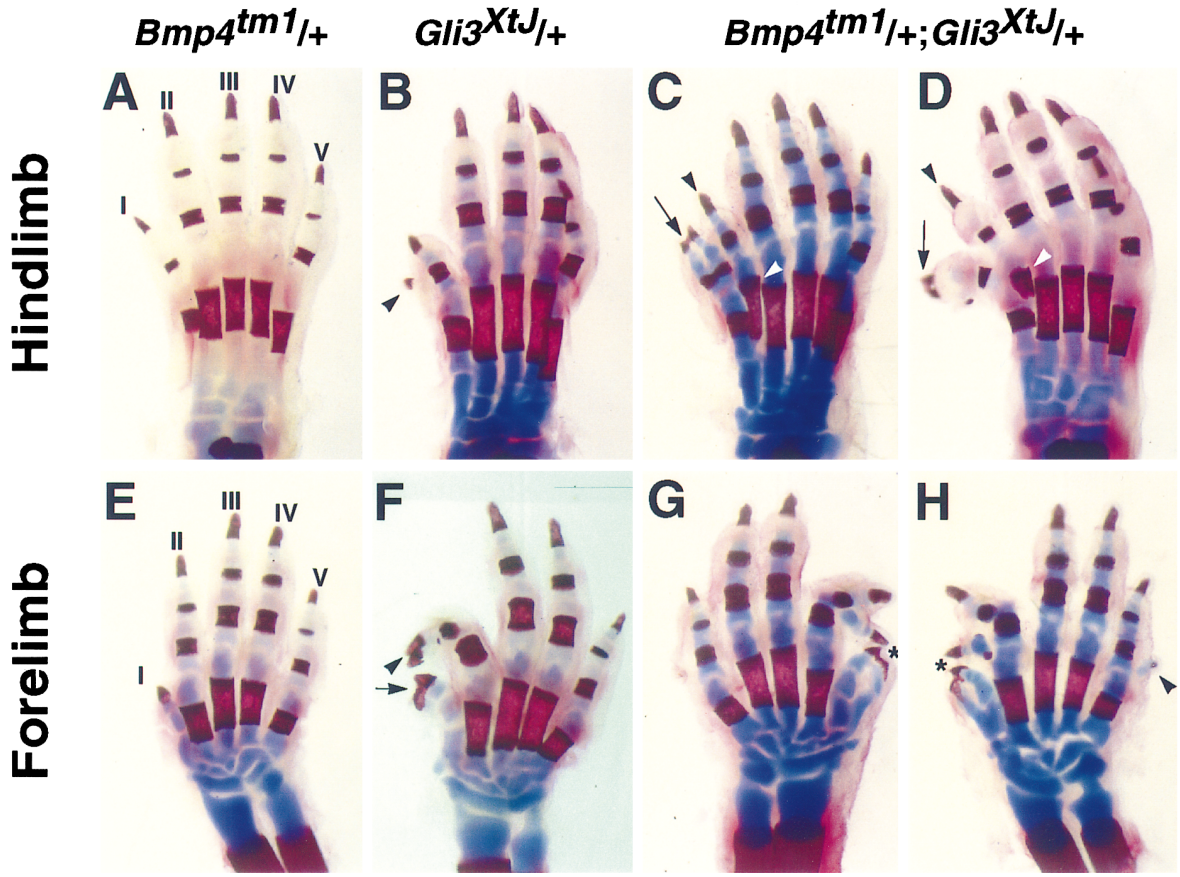


**FIG. 3.** Fore- and hindlimb defects in *Bmp4*$^{tm1}$/+, *Gli3*$^{Xtj}$/+, and *Bmp4*$^{tm1}$/+; *Gli3*$^{Xtj}$/+ newborn mice on the C57BL/6 background. All panels show dorsal views of limbs after staining with alizarin red and Alcian blue. (A and E) These *Bmp4*$^{tm1}$/+ fore- and hindlimbs show wild-type morphology. (B) *Gli3*$^{Xtj}$ heterozygotes display anterior ossified nubbins at high frequency (arrowhead in B). (C and D) Double *Bmp4*$^{tm1}$; *Gli3*$^{Xtj}$ heterozygous hindlimbs show an ectopic metatarsal (white arrowhead in C and D) that extends an ectopic biphalangeal digit (black arrowhead in C and D). In addition, polysyndactyly (arrow in C) and polydactyly (arrow in D) of digit I are observed. (F) In *Gli3*$^{Xtj}$/+ forelimbs, ventral or ventrolateral flexure of digit II is often observed, with infrequent duplications of the distal phalange (arrowhead in F). The distal phalange of the rudimentary thumb is also thickened and broadened (arrow in F). (G and H) Double heterozygotes display enhanced forelimb abnormalities. Left and right forelimbs of one affected specimen are shown in G and H. The cartilaginous axis of digit I is bifurcated, with syndactyly of the distal phalange (asterisk in G and H). Digit II is shifted laterally and is bifurcated distal to either P2 (G) or the metatarsal (H). Ectopic posterior nubbins are also observed (arrowhead in H).

*al.*, 1993; Chen *et al.*, 1996; for review Davidson, 1995). *Msx1* and *Msx2* are expressed in nearly identical domains within the developing limb bud and in regions that overlap significantly with *Bmp4* (Ros *et al.*, 1994). We therefore analyzed *Msx1* and *Msx2* expression in *Gli3*$^{Xtj}$ and *Alx4*$^{tm1}$ homozygous limbs. At 12.0–12.5 days p.c. (Figs. 5D–5I), *Msx1* and *Msx2* were expressed in both the mesenchyme and AER of the wild-type limb bud. In *Gli3*$^{Xtj}$ and *Alx4*$^{tm1}$ homozygous limb buds, the distribution and level of *Msx1* and *Msx2* transcripts were maintained even as the hyperphalangeal mutant phenotypes became morphologically distinguishable, suggesting that neither Gli3 nor Alx4 positively regulate *Msx* expression. Similar results were seen in limb buds from 10.5 to 13.5 days p.c.

### *Sonic Hedgehog Expression in Bmp4*$^{tm1}$*; Gli3*$^{Xtj}$ *and Bmp4*$^{tm1}$*; Alx4*$^{tm1}$ *Double Heterozygous Limbs*

Ectopic *Sonic hedgehog* (*Shh*) expression has been observed by *in situ* hybridization in the anterior mesenchyme of both *Gli3*$^{Xtj}$/*Gli3*$^{Xtj}$ and *Alx4*$^{tm1}$/*Alx4*$^{tm1}$ mutant limbs at 11.5 days p.c. (Masuya *et al.*, 1995, 1997; Büscher *et al.*, 1997; Qu *et al.*, submitted for publication). We therefore investigated whether the enhanced polydactylous phenotypes of double heterozygotes were similarly associated with ectopic *Shh* expression. In both *Bmp4*$^{tm1}$/+; *Alx4*$^{tm1}$/+ and *Bmp4*$^{tm1}$/+; *Gli3*$^{Xtj}$/+ mutant embryos, a small focus of *Shh* expression was sometimes seen in the anteroproximal mesenchymal cells of either the left or right hindlimb

**TABLE 4**
Genotypes of Offspring from the *Bmp4*$^{tm1}$ × *Alx4*$^{tm1}$ Cross

| *Bmp4*$^{tm1}$ × Alx4$^{tm1}$ | |
|---|---|
| Genotype[a] | Number (%)[b] |
| +/+; +/+ | 11 (28%) |
| +/+; *Alx4*$^{tm1}$ | 10 (25%) |
| *Bmp4*$^{tm1}$/+; +/+ | 7 (17%) |
| *Bmp4*$^{tm1}$/+; *Alx4*$^{tm1}$/+ | 12 (30%) |
| Total | 40 |

[a] Tail biopsies were collected between birth and P2 for genotyping.

[b] The data shown here represent the combined number of pups born in the 129.B6-*Bmp4*$^{tm1}$ (N2) × 129/J-*Alx4*$^{tm1}$/+ and 129/Sv-*Bmp4*$^{tm1}$/+ × 129/J-*Alx4*$^{tm1}$/+ crosses. Consistent with the data obtained from the *Bmp4*$^{tm1}$ × *Gli3*$^{Xtj}$ cross (Table 3), approximately equal numbers of *Bmp4*$^{tm1}$ heterozygotes and wild-type pups were genotyped at birth.

bud at 11.5 days p.c. (Figs. 6C and 6D). In both double mutants, the expression level of ectopic *Shh* was markedly lower than the wild-type level in the posterior (Figs. 6A, 6C, and 6D). Since the double heterozygous phenotypes occurred bilaterally, our detection of unilateral ectopic anterior *Shh* patches could mean that the level of *Shh* RNA in the contralateral limb was below the limit of detection by whole-mount *in situ* hybridization or that one hindlimb bud was developmentally more advanced than the other.

### *Cell Death in Bmp4*$^{tm1}$/+; *Gli3*$^{Xtj}$/+ *Limb Buds*

There is considerable evidence that apoptosis is an important patterning process in the anterior of the developing limb (Saunders and Fallon, 1967; Hinchliffe, 1982; Milaire and Rooze, 1983; Milaire, 1992). To examine the distribution of apoptotic cells in *Bmp4*$^{tm1}$/+; *Gli3*$^{Xtj}$/+ embryos, we stained 12.5-day-p.c. limbs with Nile blue sulfate, which is readily taken up by apoptotic cells (Fig. 7). In wild-type hindlimb buds, two characteristic domains of mesodermal cell death were observed: a region of cells which extended postaxially along the length of presumptive digit V to digit IV and a second strongly staining region in the anteroproximal involuting AER, as well as in the preaxial subridge mesoderm. The preaxial mesodermal apoptotic area was entirely absent in *Gli3*$^{Xtj}$; *Bmp4*$^{tm1}$ double heterozygous hindlimbs, whereas postaxial apoptotic cells were found in the normal number and in the appropriate distribution.

## DISCUSSION

### *A Haploinsufficient Bmp4*$^{tm1}$ *Phenotype on the C57BL/6 Background*

In this paper, we provide evidence that mice with only one functional copy of *Bmp4* show specific developmental defects in a subset of the organs and tissues that normally express the gene during embryogenesis (e.g., kidney, limb, eye, anterior craniofacial region). These heterozygous phenotypes occur at low penetrance and, to date, only on a predominantly C57BL/6 genetic background. The overall conclusion from these findings is that a single copy of *Bmp4* cannot generate enough active protein from the relevant sources to rise above the threshold necessary for achieving an appropriate biological response in target cells.

There are several possible reasons why the heterozygous null mutant phenotypes are seen only on a predomi-

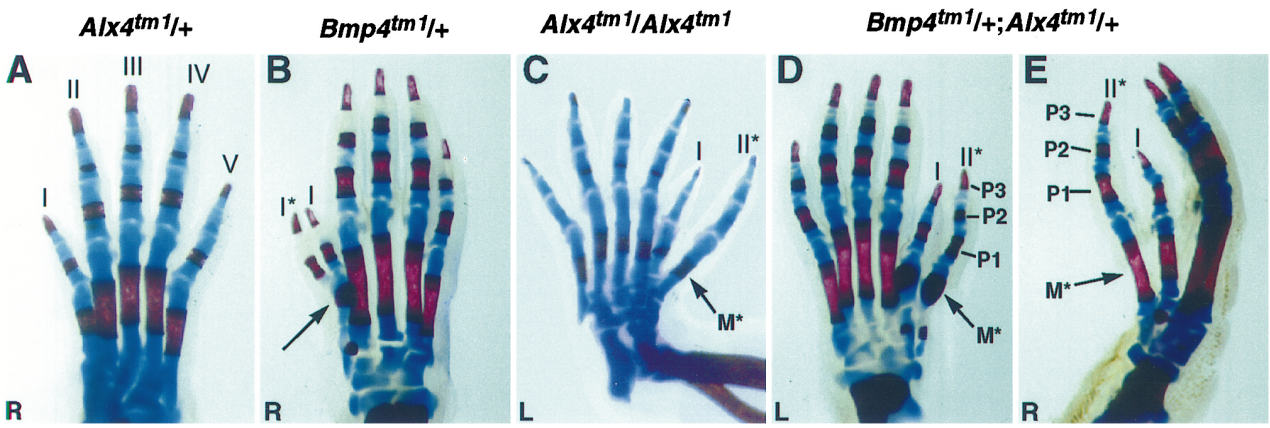


**FIG. 4.** Hindlimb defects in *Bmp4*$^{tm1}$/+, *Alx4*$^{tm1}$/+, *Alx4*$^{tm1}$/*Alx4*$^{tm1}$, and *Bmp4*$^{tm1}$/+; *Alx4*$^{tm1}$/+ newborn mice on a (129 × C57BL/6) background. All panels show dorsal views of left (L) or right (R) hindlimbs after double staining with alizarin red and Alcian blue. (A) Heterozygous *Alx4*$^{tm1}$/+ hindlimbs show wild-type morphology. (B) An extra anterior biphalangeal digit (I*), extending from a common metatarsal (arrow), is observed infrequently among newborn *Bmp4*$^{tm1}$ heterozygotes. (C) Extra anterior triphalangeal digits (II*) that extend from a duplicated metatarsal (M*) are observed in all *Alx4*$^{tm1}$ homozygous newborns. (D and E) In double *Bmp4*$^{tm1}$; *Alx4*$^{tm1}$ heterozygotes, ectopic anterior metatarsals (M* in D and E) extend triphalangeal digits on both the left and right hindlimbs. P1–P3 represent the digital phalanges.

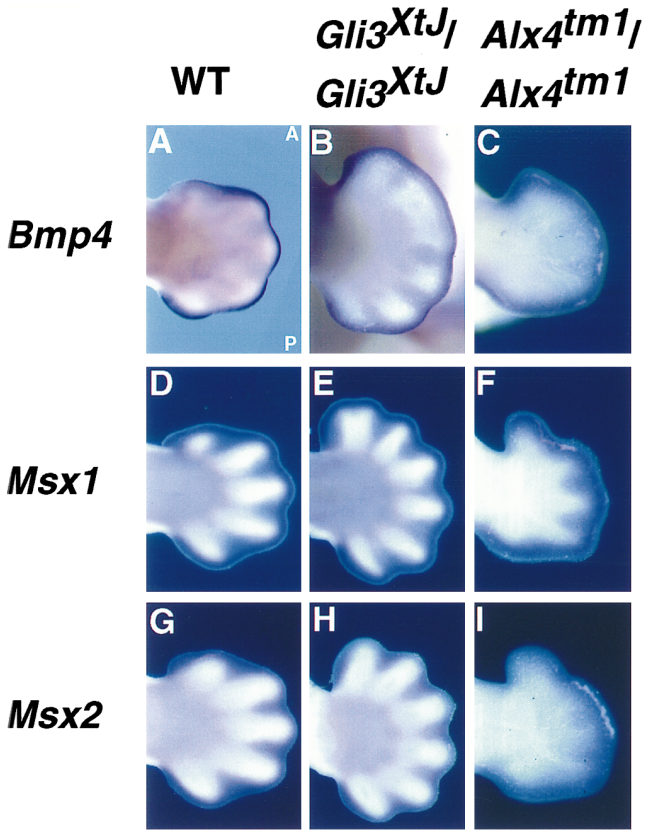


**FIG. 5.** The expression of *Bmp4*, *Msx1*, and *Msx2* in wild-type, *Gli3*$^{XtJ}$/*Gli3*$^{XtJ}$, and *Alx4*$^{tm1}$/*Alx4*$^{tm1}$ developing limbs. (A, D, G) 12.5 days p.c. wild type, (B, E, H) 12.5 days p.c. *Gli3*$^{XtJ}$/*Gli3*$^{XtJ}$, and (C, F, I) 12.0-12.5 days p.c. *Alx4*$^{tm1}$/*Alx4*$^{tm1}$ limb buds. At 12.5 days p.c., *Bmp4* expression is observed in the distal mesoderm underneath the involuting AER and outlines the tips of the forming digits (A). *Msx1* and *Msx2* are expressed in similar domains within the mesoderm of the wild-type limb bud, particularly in the interdigital regions. *Msx2* expression is also observed weakly in the AER (not in focus in G, H, I). In both *Gli3*$^{XtJ}$ homozygous and *Alx4*$^{tm1}$ homozygous limbs, severe morphological malformations are apparent at 12.0–12.5 days p.c. (B, C, E, F, H, I). However, there are no obvious differences in the distributions of *Bmp4*, *Msx1*, or *Msx2* transcripts in the homozygous mutant limbs. A, anterior; P, posterior.

nantly C57BL/6 background. Strain-dependent differences in the activity of genes encoding extracellular proteins that bind and inactivate BMP4 (for example, noggin or chordin) may effectively reduce the amount of available ligand (Piccolo *et al.*, 1996; Zimmerman *et al.*, 1996). Alternatively, C57BL/6-specific alleles of genes encoding BMP receptors or downstream effectors may be differentially active between different mouse strains. Similarly, genes encoding proteins with partially overlapping functions for BMP4 (e.g., BMP2) may be less transcriptionally active in C57BL/6. Any of these effects, which are not necessarily exclusive, may cause stochastic local variations in active BMP4 protein levels at critical stages during the development of specific organs.

Heterozygous phenotypes have also been reported for null mutations in the *Bmp5* gene on some genetic backgrounds, which suggests that haploinsufficiency is a general feature of null mutations in genes encoding BMP family members, not only in *Drosophila* but also in mammals (Green, 1968).

### *Genetic Interaction between Bmp4$^{tm1}$ and Gli3$^{XtJ}$*

Our results demonstrate striking polydactylous phenotypes of mice doubly heterozygous for mutations in *Bmp4* and *Gli3*. *Bmp4*$^{tm1}$/+ heterozygotes show incompletely penetrant preaxial polydactyly with, in the most severe cases (70% of affected individuals), one ectopic triphalangeal digit exclusively on the right hindfoot. The most severe defect in the hindfeet of *Gli3*$^{XtJ}$ heterozygotes is a biphalangeal digit. This is seen in only 8% of the affected individuals, while the most common heterozygous phenotype is a preaxial ossified nubbin (58%). In contrast, double *Bmp4*$^{tm1}$; *Gli3*$^{XtJ}$ show bilateral hindlimb phenotypes that are more severe than that of either heterozygote alone. Both hindfeet of all double heterozygotes show two to three ectopic bi- or triphalangeal digits, an ectopic metatarsal, soft tissue syndactyly, and overgrowth and sometimes fusion of the bones of the ectopic digits and metatarsals.

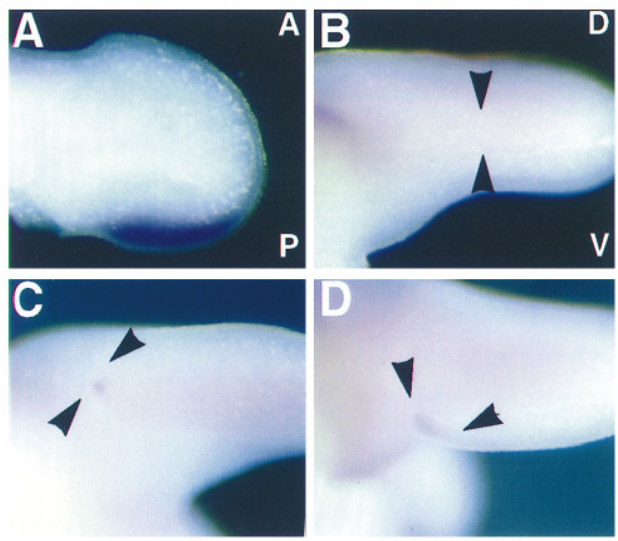


**FIG. 6.** The expression of *Shh* in wild-type, *Bmp4*$^{tm1}$/+; *Gli3*$^{XtJ}$/+, and *Bmp4*$^{tm1}$/+; *Alx4*$^{tm1}$/+ hindlimb buds. (A) At 11.5 days p.c., *Shh* expression is exclusively observed in the mesenchyme along the posterior margin of wild-type limb buds. An anterior view of a wild-type limb bud confirms the absence of *Shh* in the anterior mesenchyme (black arrowheads). In both *Bmp4*$^{tm1}$; *Alx4*$^{tm1}$ (C) and *Bmp4*$^{tm1}$; *Gli3*$^{XtJ}$ (D) double heterozygotes, a small ectopic anterior domain of low level *Shh* expression is observed (black arrowheads in C and D). A, anterior; P, posterior; D, dorsal; V, ventral.

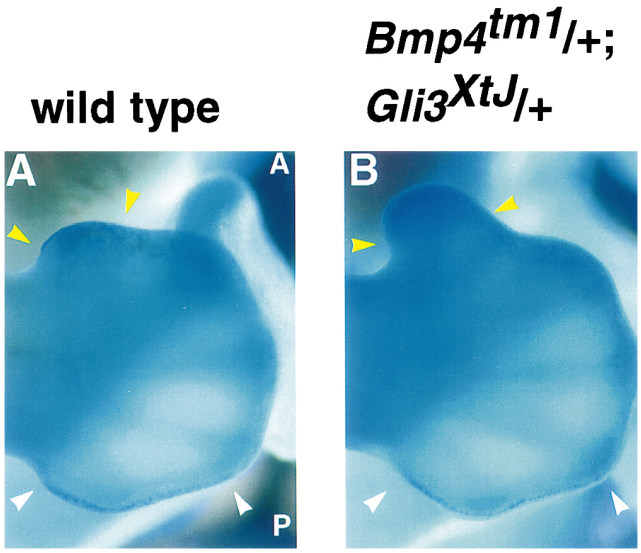


**FIG. 7.** Apoptosis patterns in wild-type and $Bmp4^{tm1}/+$; $Gli3^{Xtj}/+$ hindlimb buds. A population of Nile blue-positive apoptotic cells in the subridge mesoderm extends along the postaxial margin of wild-type and $Bmp4^{tm1}/+$; $Gli3^{Xtj}/+$ hindlimb buds (extremities indicated by white arrowheads in A and B). A second population of apoptotic cells is observed in the anteroproximal AER and underlying preaxial subridge mesoderm (yellow arrowheads in A), but is entirely absent from the $Bmp4^{tm1}$; $Gli3^{Xtj}$ double heterozygous hindlimb (yellow arrowheads in B). A, anterior; P, posterior.

There are two possible interpretations of the results described above. In the first case (direct genetic interaction model), *Bmp4* and *Gli3* may be components of the same intracellular signaling pathway. For example, Gli3 may positively regulate *Bmp4* expression, BMP4 may regulate *Gli3* expression, or Gli3 may be a component of the BMP4 downstream signaling cascade, regulating the expression of such putative BMP4 target genes as *Msx1* and *Msx2*. Alternatively, BMP4 and Gli3 may both independently regulate different processes affecting limb growth and patterning. As discussed below, our results do not at present allow us to unequivocally distinguish between these possibilities. However, our results do provide the first *in vivo* genetic evidence for a role for BMP4 in limb growth and patterning; the fact that our results are not yet easily accounted for by current models of limb development must only serve to stimulate further experimentation.

### *Direct Interaction Model*

*Gli3* and *Bmp4* are expressed in the same region of mesenchyme in the anterior limb bud at 10.5 and 11.5 days p.c. (Hui and Joyner, 1993; Hui *et al.*, 1994; Francis *et al.*, 1994; Hogan, 1996; Büscher *et al.*, 1997; Masuya *et al.*, 1997; Mo *et al.*, 1997), and there is overlap in expression in the posterior mesenchyme earlier in development (Marigo *et al.*, 1996; N.R.D. and B.L.M.H., unpublished observations). However, our results, and those of others, have failed to show an obvious decrease in *Bmp4* expression in $Gli3^{Xtj}/Gli3^{Xtj}$ limbs between 10.5 and 13.5 days p.c. (Fig. 5; Büscher *et al.*, 1997). It could, of course, be argued that other *Gli* genes (*Gli* and *Gli2*) compensate for the absence of *Gli3* in regulating *Bmp4* expression, resulting in only a slight decrease in *Bmp4* expression, not detectable by *in situ* hybridization. This explanation would, at least, imply that *Gli* genes normally positively regulate or maintain *Bmp4* expression. Similar arguments can be made for the absence of any significant decrease in *Msx1* and *Msx2* expression in $Gli3^{Xtj}/Gli3^{Xtj}$ limbs. Because only a few $Bmp4^{tm1}$ homozygous mutants develop to the early forelimb bud stage (Winnier *et al.*, 1995), we have been unable to test whether the levels of *Gli3* RNA are significantly changed in homozygous mutant limbs, as might be expected if *Bmp4* is epistatic to *Gli3* in the limb bud mesenchyme. However, it should be noted that *Gli3* levels are reported to be lower in the posterior mesenchyme where *Bmp4* levels are high (Masuya *et al.*, 1995, 1997; Marigo *et al.*, 1996; Büscher *et al.*, 1997; N.R.D. and B.L.M.H., unpublished observations), arguing for a negative regulation of *Gli3* by BMP4.

### *Indirect Interaction Model*

An alternative, equally valid model for the synergistic effect of *Bmp4* and *Gli3* heterozygous null mutations is that these genes independently affect parallel pathways that govern anterior limb patterning. BMP4 may normally play several roles in limb patterning, including the regulation of cell death in the anterior and posterior necrotic zones and in the interdigital mesenchyme. There is considerable experimental evidence for such a role in chick limb development. For example, blocking endogenous BMP signaling with a retrovirus expressing a dominant negative type I BMP receptor in developing chick limb buds leads to suppression of mesodermal cell death, resulting in the formation of ectopic anterior bulges and persistent interdigital webbing (Zou and Niswander, 1996; Yokouchi *et al.*, 1997). In contrast, the implantation of BMP4 beads into the interdigital spaces accelerates cell death and digit emergence (Gañan *et al.*, 1996). Given these results, it is likely that BMP4 also regulates cell death in the mesoderm, particularly in the anterior and posterior necrotic zones, and in the AER of the developing mouse limb. Reduced BMP4 levels in heterozygous $Bmp4^{tm1}$ embryos may therefore increase cell numbers in the limb bud, both by reducing mesenchymal cell death and by prolonging the survival of the AER and consequently the secretion from the AER of growth-promoting FGFs. However, only in a small percentage of heterozygotes does the anterior cell population exceed the threshold for generating extra digits.

Homozygous $Gli3^{Xtj}$ mutants show enlarged, paddle-shaped limb buds, and this phenotype is associated with an upregulation of *Shh* in the anterior (~11.5 days p.c.). In

addition, transgenic mice overexpressing *Shh* under the control of the keratin 14 promoter were recently generated, and they display polydactyly that strongly resembles the hyperphalangeal phenotypes of the few *Gli3$^{XtJ}$/Gli3$^{XtJ}$* embryos that survive to late gestation or birth (Johnson, 1967; Oro *et al.*, 1997). Taken together, these observations suggest that Gli3 normally functions to repress *Shh* and that in *Gli3$^{XtJ}$* homozygous limbs the ectopic Shh stimulates the overproliferation of the limb mesoderm. Similarly, in *Gli3$^{XtJ}$* heterozygotes, the amount of active Gli3 protein is reduced, relieving, if only slightly, *Shh* repression and consequently leading to an increased mesodermal cell mass and minor preaxial digit abnormalities. The combination of increased cell proliferation and decreased cell death in the anterior of *Bmp4$^{tm1}$; Gli3$^{XtJ}$* double heterozygous limbs may therefore result in a local accumulation of mesoderm which responds to anterior patterning signals, giving rise to ectopic digits, which may be malformed or syndactylous, and occasionally to additional skeletal elements such as metatarsals.

### *Genetic Interaction between Bmp4$^{tm1}$ and Alx4$^{tm1}$*

Both *Alx4* and *Bmp4* are expressed in the same localized region within the anterior limb bud mesenchyme at 10.5–11.0 days p.c. (Qu *et al.*, submitted for publication; N.R.D. and B.L.M.H., unpublished observations). According to the direct interaction model, it is possible that Alx4 normally positively regulates the level of *Bmp4* RNA. Using the same logic as applied above, we think that this is unlikely, since the expression patterns and levels of *Bmp4*, *Msx1*, and *Msx2* were not significantly changed in *Alx4$^{tm1}$* homozygous mutant embryos.

Alternatively, the effects of *Bmp4* and *Alx4* heterozygous null mutations in combination may allow the population of anterior mesenchymal cells to consistently exceed the threshold necessary for making extra digits. Our data and those of others suggest that both Alx4 and Gli3 are repressors of anterior Shh expression; loss-of-function mutations in either gene lead to ectopic anterior *Shh* and to overproliferation of anterior mesenchyme in homozygous limbs (Masuya *et al.*, 1995, 1997; Büscher *et al.*, 1997; Qu *et al.*, submitted for publication). Although *Alx4$^{tm1}$/+*, in contrast to *Gli3$^{XtJ}$/+*, mice are phenotypically wild type, it is still possible that an extremely low level of Shh is produced in the anterior hindlimb bud. In *Bmp4$^{tm1}$; Alx4$^{tm1}$* double heterozygous limbs, the addition of the weak Shh mitogenic signal to the reduced cell death resulting from decreased BMP4 leves promotes the formation of anterior supernumerary digits.

In conclusion, heterozygous mutations acting together in the same limb can enhance the penetrance and severity of either mutant phenotype, in some cases generating new combinatorial phenotypes. These findings have relevance for understanding variations in the phenotype of developmental mutations on different genetic backgrounds in mice and in human populations.

## ACKNOWLEDGMENTS

We thank Drs. C.-c. Hui, Christopher Wright, and Lee Niswander for generous advice and encouragement and Lucy Liaw for establishing the 1A10H line. We also thank Drs. David Threadgill, David Greenstein, and Lilliana Solnica-Krezel and laboratory colleagues for many valuable discussions and comments on the manuscript, Julie Blackwell and Lorene Batts for skilled technical assistance, and Dr. Shimian Qu for graciously providing Figure 4C. This work was supported by NIH HD28955. N.R.D. acknowledges support from the multidisciplinary Viruses, Nucleic Acids, and Cancer NIH Predoctoral Training Grant 5T32CA09385. B.L.M.H. is an Investigator of the Howard Hughes Medical Institute.

## REFERENCES

Alexandre, C., Jacinto, A., and Ingham, P. W. (1996). Transcriptional activation of *hedgehog* target genes in *Drosophila* is mediated directly by the Cubitus interruptus protein, a member of the GLI family of zinc finger DNA-binding proteins. *Genes Dev.* **10,** 2003–2013.

Barlow, A. J., and Francis-West, P. H. (1997). Ectopic application of recombinant BMP-2 and BMP-4 can change patterning of developing chick facial primordia. *Development* **124,** 391–398.

Bellusci, S., Henderson, R., Winnier, G., Oikawa, T., and Hogan, B. L. M. (1996). Evidence from normal expression and targeted misexpression that *Bone Morphogenetic Protein-4* (*Bmp-4*) plays a role in mouse embryonic lung morphogenesis. *Development* **122,** 1693–1702.

Bitgood, M. J., and McMahon, A. P. (1995). *Hedgehog* and *Bmp* genes are coexpressed at many diverse sites of cell-cell interaction in the mouse embryo. *Dev. Biol.* **172,** 126–138.

Büscher, D., Bosse, B., Heymer, J., and Rüther, U. (1997). Evidence for genetic control of *Sonic hedgehog* by *Gli3* in mouse limb bud development. *Mech. Dev.* **62,** 175–182.

Chen, Y., Bei, M., Woo, I., Satokata, I., and Maas, R. (1996). *Msx1* controls inductive signaling in mammalian tooth morphogenesis. *Development* **122,** 3035–3044.

Davidson, D. (1995). The function and evolution of *Msx* genes: Pointers and paradoxes. *Trends Genet.* **11,** 405–411.

Domínguez, M., Brunner, M., Hafen, E., and Basler, K. (1996). Sending and receiving the hedgehog signal: Control by the *Drosophila* Gli protein Cubitus interruptus. *Science* **272,** 1621–1625.

Dudley, A. T., and Robertson, E. J. (1997). Overlapping expression domains of BMP family members potentially account for the limited defects in BMP7 deficient embryos. *Dev. Dyn.* **208,** 349–362.

Erickson, R. P. (1996). Mouse models of human genetic disease: Which mouse is more like a man? *BioEssays* **18,** 993–998.

Ferguson, E. L., and Anderson, K. V. (1992a). *decapentaplegic* acts as a morphogen to organize dorsal-ventral pattern in the *Drosophila* embryo. *Cell* **71,** 451–461.

Ferguson, E. L., and Anderson, K. V. (1992b). Localized enhancement and repression of the activity of the TGF-$\beta$ family member, *decapentaplegic,* is necessary for dorsal–ventral pattern formation in the *Drosophila* embryo. *Development* **114,** 583–597.

Francis, P. H., Richardson, M. K., Brickell, P. M., and Tickle, C. (1994). Bone morphogenetic proteins and a signalling pathway that controls patterning in the developing limb bud. *Development* **120,** 209–218.

Furuta, Y., Piston, D. W., and Hogan, B. L. M. (1997). Bone morphogenetic proteins (BMPs) as regulators of dorsal forebrain development. *Development* **124,** 2203–2212.

Gañan, Y., Macias, D., Duterque-Coquillaud, M., Ros, M. A., and Hurle, J. M. (1996). Role of TGF$\beta$s and BMPs as signals controlling the position of the digits and the areas of interdigital cell death in the developing chick limb autopod. *Development* **122,** 2349–2357.

Goto, S., and Hayashi, S. (1997). Specification of the embryonic limb primordium by graded activity of Decapentaplegic. *Development* **124,** 125–132.

Green, M. C. (1957). Modifiers of the pleiotropic effects of the *short ear* gene in the mouse. *J. Hered.* **48,** 205–212.

Green, M. C. (1968). Mechanism of the pleitropic effects of the *short ear* mutant gene in the mouse. *J. Exp. Zool.* **167,** 129–150.

Gurdon, J. B., Harger, P., Mitchell, A., and Lemaire, P. (1994). Activin signalling and response to a morphogen gradient. *Nature* **371,** 487–492.

Hepker, J., Wang, Q.-T., Motzny, C. K., Holmgren, R., and Orenic, T. V. (1997). *Drosophila cubitus interruptus* forms a negative feedback loop with *patched* and regulates expression of Hedgehog target genes. *Development* **124,** 549–558.

Hinchliffe, J. R. (1982). Cell death in vertebrate limb morphogenesis. *Prog. Anat.* **2,** 1–17.

Hogan, B. L. M. (1996). Bone morphogenetic proteins: multifunctional regulators of embryonic development. *Genes Dev.* **10,** 1580–1594.

Hui, C.-c., and Joyner, A. L. (1993). A mouse model of Greig cephalopolysyndactyly syndrome: the *extra-toes*$^{J}$ mutation contains an intragenic deletion of the *Gli3* gene. *Nature Genet.* **3,** 241–246.

Hui, C.-c., Slusarski, D., Platt, K. A., Holmgreen, R., and Joyner, A. L. (1994). Expression of three mouse homologs of the *Drosophila* segment polarity gene *cubitus interruptus, Gli, Gli-2* and *Gli-3,* in ectoderm- and mesoderm-derived tissues suggests multiple roles during postimplantation development. *Dev. Biol.* **162,** 402–413.

Irish, V. F., and Gelbart, W. M. (1987). The *decapentaplegic* gene is required for doral-ventral pattering of the *Drosophila* embryo. *Genes Dev.* **1,** 868–879.

Johnson, D. R. (1967). *Extra-toes:* A new mutant gene causing multiple abnormalities in the mouse. *J. Embryol. Exp. Morphol.* **17,** 543–581.

Johnson, D. R. (1969). *Brachyphalangy,* an allele of *extra-toes* in the mouse. *Genet. Res. Camb.* **13,** 275–280.

Jones, C. M., Armes, N., and Smith, J. C. (1996). Signalling by TGF-$\beta$ family members: short-range effects of Xnr-2 and BMP-4 contrast with the long-range effects of activin. *Curr. Biol.* **6,** 1468–1475.

Jones, C. M., Lyons, K. M., and Hogan, B. L. M. (1991). Involvement of *Bone Morphogenetic Protein-4* (*BMP-4*) and *Vgr-1* in morphogenesis and neurogenesis in the mouse. *Development* **111,** 531–542.

King, J. A., Marker, P. C., Seung, K. S., and Kingsley, D. M. (1994). BMP5 and the molecular, skeletal, and soft-tissue alterations in *short ear* mice. *Dev. Biol.* **166,** 112–122.

Kingsley, D. M., Bland, A. E., Grubber, J. M., Marker, P. C., Russell, L. B., Copeland, N. G., and Jenkins, N. A. (1992). The mouse *short ear* skeletal morphogenesis locus is associated with defects in a bone morphogenetic member of the TGF$\beta$ superfamily. *Cell* **71,** 399–410.

Kinzler, K. W., Ruppert, J. M., Bigner, S. H., and Vogelstein, B. (1988). The *GLI* gene is a member of the *Kruppel* family of zinc finger proteins. *Nature* **332,** 371–374.

Laird, P. W., Zijderveld, A., Linders, K., Rudnicki, M. A., Jaenisch, R., and Berns, A. (1991). Simplified mammalian DNA isolation procedure. *Nucleic Acids Res.* **19,** 4293.

Lecuit, T., Brook, W. J., Ng, M., Calleja, M., Sun, H., and Cohen, S. (1996). Two distinct patterning mechanisms for long-range patterning by Decapentaplegic in the *Drosophila* wing. *Nature* **381,** 387–393.

Marigo, V., Johnson, R. L., Vortkamp, A., and Tabin, C. J. (1996). Sonic hedgehog diferentially regulates expression of *GLI* and *GLI3* during limb development. *Dev. Biol.* **180,** 273–283.

Masuya, H., Sagai, T., Moriwaki, K., and Shiroishi, T. (1997). Multigenic control of the localization of the zone of polarizing activity in limb morphogenesis in the mouse. *Dev. Biol.* **182,** 42–51.

Masuya, H., Sagai, T., Wakana, S., Moriwaki, K., and Shiroishi, T. (1995). A duplicated zone of polarizing activity in polydactylous mouse mutants. *Genes Dev.* **9,** 1645–1653.

McLeod, M. J. (1980). Differential staining of cartilage and bone in whole mouse fetuses by alcian blue and alizarin red S. *Teratology* **22,** 229–301.

Milaire, J. (1992). A new interpretation of the necrotic changes occurring in the developing limb bud paddle of mouse embryos based upon recent observations in four different phenotypes. *Int. J. Dev. Biol.* **36,** 169–178.

Milaire, J., and Rooze, M. (1983). Hereditary and induced modifications of the normal necrotic patterns in the developing limb buds of the rat and mouse: facts and hypotheses. *Arch. Biol.* **94,** 459–490.

Mo, R., Freer, A. M., Zinyk, D. L., Crackower, M. A., Michaud, J., Heng, H. H.-Q., Chik, K. W., Shi, X.-M., Tsui, L.-C., Cheng, S. H., Joyner, A. L., and Hui, C.-c. (1997). Specific and redundant functions of *Gli2* and *Gli3* zinc finger genes in skeletal patterning and development. *Development* **124,** 113–123.

Nellen, D., Burke, R., Struhl, G., and Basler, K. (1996). Direct and long-range action of a DPP morphogen gradient. *Cell* **85,** 357–368.

Orenic, T. V., Slusarski, D. C., Kroll, K. L., and Holmgren, R. A. (1990). Cloning and characterization of the segment polarity gene *cubitus interruptus Dominant* of *Drosophila. Genes Dev.* **4,** 1053–1067.

Oro, A. E., Higgins, K. M., Hu, Z., Bonifas, J. M., Epstein, E. H., Jr., and Scott, M. P. (1997). Basal cell carcinomas in mice overexpressing Sonic hedgehog. *Science* **276,** 817–821.

Piccolo, S., Sasai, Y., Lu, B., and De Robertis, E. M. (1996). Dorsoventral patterning in *Xenopus:* inhibition of ventral signals by direct binding of chordin to BMP4. *Cell* **86,** 589–598.

Raftery, L. A., Twombly, V., Wharton, K., and Gelbart, W. M. (1995). Genetic screens to identify elements of the *decapentaplegic* signaling pathway in *Drosophila. Genetics* **139,** 214–254.

Reilly, K. M., and Melton, D. A. (1996). Short-range signaling by candidate morphogens of the TGF$\beta$ Family and evidence for a relay mechanism of induction. *Cell* **86,** 743–754.

Ros, M. A., Macias, D., Fallon, J. F., and Hurle, J. M. (1994). Formation of extra digits in the interdigital spaces of the chick leg bud is not preceded by changes in the expression of the *Msx* and *Hoxd* genes. *Anat. Embryol.* **190,** 375–382.

Ruppert, J. M., Kinzler, K. W., Wong, A. J., Bigner, S. H., Kao, F.-T., Law, M. L., Seuanez, H. N., O'Brien, S. J., and Vogelstein, B.

(1988). The *GLI*-kruppel family of human genes. *Mol. Cell Biol.* **8,** 3104–3113.

Saunders, J. W., and Fallon, J. F. (1967). Cell death in morphogenesis. *In* ''Major Problems in Developmental Biology'' (M. Locke, Ed.), pp. 289–314. Academic Press, New York.

Schimmang, T., Lemaistre, M., Vortkamp, A., and Rüther, U. (1992). Expression of the zinc finger gene *Gli3* is affected in the morphogenetic mouse mutant *extra-toes* (*Xt*). *Development* **116,** 799–804.

Schimmang, T., Oda, S.-I., and Rüther, U. (1994). The mouse mutant *Polydactyly Nagoya* (*Pdn*) defines a novel allele of the zinc finger gene *Gli3*. *Mamm. Genome* **5,** 384–386.

Selby, P. B. (1987). A rapid method for preparing high quality alizarin stained skeletons of adult mice. *Stain Technol.* **62,** 143–146.

Silver, L. M. (1995). Mouse genetics: Concepts and applications. Oxford University Press, Inc., New York.

Singer, M. A., Penton, A., Twombly, V., Hoffmann, F. M., and Gelbart, W. M. (1997). Signaling through both type I DPP receptors is required for anterior-posterior patterning of the entire *Drosophila* wing. *Development* **124,** 79–89.

Soriano, P., Montgomery, C., Geske, R., and Bradley, A. (1991). Targeted disruption of the *c-src* proto-oncogene leads to osteoporosis in mice. *Cell* **64,** 693–702.

St. Johnston, R. D., and Gelbart, W. B. (1987). *Decapentaplegic* transcripts are localized along the dorsal-ventral axis of the *Drosophila* embryo. *EMBO J.* **6,** 2785–2791.

Vainio, S., Karavanova, I., Jowett, A., and Thesleff, I. (1993). Identification of BMP-4 as a signal mediating secondary induction between epithelial and mesenchymal tissues during early tooth development. *Cell* **75,** 45–58.

Wharton, K. A., Ray, R. P., and Gelbart, W. M. (1993). An activity gradient of *decapentaplegic* is necessary for the spcification of dorsal pattern elements in the *Drosophila* embryo. *Development* **117,** 807–822.

Winnier, G., Blessing, M., Labosky, P. A., and Hogan, B. L. M. (1995). Bone morphogenetic protein-4 is required for mesoderm formation and patterning in the mouse. *Genes Dev.* **9,** 2105–2116.

Winter, R. M. (1996). Analysing human developmental abnormalities. *BioEssays* **18,** 965–971.

Yokouchi, Y., Sakiyama, J.-i., Kameda, T., Iba, H., Suzuki, A., Ueno, N., and Kuroiwa, A. (1996). BMP-2/-4 mediate programmed cell death in chicken limb buds. *Development* **122,** 3725–3734.

Zimmerman, L. B., De Jesús-Escobar, J. M., and Harland, R. M. (1996). The Spemann organizer signal noggin binds and inactivates Bone Morphogenetic Protein 4. *Cell* **86,** 599–606.

Zou, H., and Niswander, L. (1996). Requirement for BMP signaling in interdigital apoptosis and scale formation. *Science* **272,** 738–741.

Received for publication May 13, 1997
Accepted June 12, 1997